The Triple Spar campaign: Model tests of a 10MW floating wind turbine with waves, wind and pitch control

Bredmose, Henrik; Lemmer, F.; Borg, Michael; Pegalajar Jurado, Antonio Manuel; Mikkelsen, Robert Flemming; Larsen, T. Stoklund; Fjelstrup, T.; Yu, Wenye; Lomholt, Anders Kjær; Boehm, L.; Armendariz, J. Azcona

Published in:
Energy Procedia

Link to article, DOI:
10.1016/j.egypro.2017.10.334

Publication date:
2017

Document Version
Publisher's PDF, also known as Version of record

Available online at www.sciencedirect.com

ScienceDirect

Energy Procedia 137 (2017) 58–76

Energy Procedia

www.elsevier.com/locate/procedia

14th Deep Sea Offshore Wind R&D Conference, EERA DeepWind'2017, 18-20 January 2017, Trondheim, Norway

The Triple Spar campaign: Model tests of a 10MW floating wind turbine with waves, wind and pitch control

H. Bredmose[a,*], F. Lemmer[b], M. Borg[a], A. Pegalajar-Jurado[a], R.F. Mikkelsen[a], T. Stoklund Larsen[a], T. Fjelstrup[a], W. Yu[b], A.K. Lomholt[a], L. Boehm[a], J. Azcona Armendariz[c]

[a]*DTU Wind Energy, Nils Koppels Allé Building 403, DK-2800 Kgs. Lyngby, Denmark*
[b]*University of Stuttgart, Stuttgart Wind Energy, Allmandring 5b, 70569 Stuttgart, Germany*
[c]*CENER, Ciudad de la Innovación, no. 7, 31621 Sarriguren (Navarra), Spain*

Abstract

Results of a test campaign for a floating wind turbine in simultaneous wind and wave forcing at scale 1:60 are presented. The floater is the Triple Spar floater, a hybrid between a spar buoy and a semi submersible tri-floater, tested here for the first time. The turbine is a model scale version of the DTU 10 MW reference wind turbine, which, also for the first time, is tested with active blade pitch control. The tests focus on the effects of aerodynamic damping and interaction effects between the wind forcing, wave forcing and the blade pitch control algorithm. Special focus is devoted to the instability of the platform pitch natural mode, that can occur if a standard land-based controller is applied.

Results of three control strategies are reported: Fixed blade pitch, a standard land-based controller, and a tuned controller designed to eliminate the instability. Special rotor ID tests were carried out to characterize the rotor and identify the control parameters. Results for regular waves, focused wave groups, a wind-only test and irregular waves are presented in terms of time series, power spectra and exceedance probability plots. Among the key results are the wind-induced steady offset of floater pitch and surge and the aerodynamic damping of the floater pitch motion. Further, a clear example of the onset of unstable motion at the platform natural pitch frequency is provided along with a detailed analysis of the dynamic response for irregular wave conditions with the three control strategies. The paper ends with the first results of numerical re-modelling of the response for a waves-only test. A good match is found, thus encouraging further work in this direction.

Peer-review under responsibility of SINTEF Energi AS.

Keywords: Floating wind turbines; blade pitch; control; experimental analysis; numerical modelling

* Corresponding author.
E-mail address: hbre@dtu.dk

1876-6102
Peer-review under responsibility of SINTEF Energi AS.
10.1016/j.egypro.2017.10.334

1. Introduction

Floating wind turbines are subject to forces from wind, waves and mooring. While these effects are generally nonlinear, for example through dependence of the turbines instantaneous position, the motion response is further affected by interaction effects between them. Two very important effects in this regard are aerodynamic damping and the controller action, which both have a strong impact on the structural loads. The aerodynamic damping and possibly other aerodynamic coupling effects is the main reason for carrying out model scale tests for floating wind turbines that combine wind and wave forcing. Although the aerodynamics in such tests is associated with strongly reduced Reynolds numbers and usually requires a re-design of the turbine rotor, such tests give insight into the damping effects and allows validation of numerical models. An important next step, however, is the inclusion of active blade pitch control to also model the thrust effects from the dynamic change of blade pitch that a real prototype turbine would experience. For floating wind turbines, this aspect is even more important than for land-based turbines, since a wrongly tuned controller might lead to resonant amplification of platform pitch motion at the platform pitch natural frequency.

The present paper describes a recent test campaign carried out by DTU, University of Stuttgart and CENER for a floating wind turbine in simultaneous wind and waves and with active blade pitch control. The purpose of the test campaign was to study and quantify the interaction effects related to aerodynamic damping and especially interaction with the controller. To this end five controllers were implemented and tested. Further objectives were to obtain physical test data for the newly designed INNWIND.EU Triple Spar floater [1;2] and produce a data base for validation of aero-elastic models. Finally, as the turbine tower was scaled elastically, the tests also provides insight into the level of tower excitation from wind and waves.

Laboratory tests with floating wind turbines have been the subject of several research projects and commercial projects in recent years. The HyWind concept was tested at Marintek, Norway, in 2005 in combined wind and waves and control. The papers of Skaare et al.[3];Nielsen et al.[4] outlines the campaign. More recently, the DeepCWind consortium lead by University of Maine carried out model tests at MARIN, The Netherlands, with a 1:45 scaled model of the NREL 5MW reference turbine [5;6]. The first campaign of 2012 involved tests for a semi-submersible platform, a tension leg platform and a spar floater with a geometrically scaled rotor. Due to the low Reynolds number in the lab conditions, this rotor was not able to deliver the required scaled thrust. However, this issue was addressed in the tests by increasing the corresponding wind speed to yield the appropriate thrust. Given the drawbacks of this approach, for a subsequent campaign in 2013 [7] the rotor was re-designed to yield the correct scaled thrust without the need of increasing the wind speed. The rotor and turbine is denoted the Marin Stock turbine and has been used in a number of subsequent tests.

Since the HyWind model tests, only few experimental campaigns have included active control of the blade pitch. In a poster at EWEA Offshore 2015, Karikomi et al.[8] reported tests in a small water tank of a spar-type turbine. The results include clear measurements of platform pitch instability above rated wind speed, which occur for land-based controller settings. They also demonstrated how a tuned controller made the system stable. Recently Goupee et al.[9] reported model tests at Marin, also with active blade pitch control. The paper demonstrates how different controller settings affect the natural platform pitch frequency and compares power spectra of platform motion for four different control strategies. Further work at Marin has been conducted by Savenije[10] and within the Lions Hat JIP project of Marin and ECN.

At DTU, scale tests at 1:200 with a re-designed rotor were carried out in 2012 for a TLP configuration [11]. A later campaign was carried out at DHI Denmark [12;13] with a 1:60 scaled model of the DTU 10MW reference wind turbine [14] on a specially designed TLP floater. The rotor was redesigned to deliver the right Froude scalend thrust at the low Reynolds number, see Mikkelsen[15], and operated at fixed speed and blade pitch. The tests were part of the INNWIND.EU project, and extended an earlier campaign of Sandner et al.[16] for a semi-submersible configuration.

The present test campaign extends the work of Bredmose et al.[12] by inclusion of active blade pitch control and adoption of the newly designed Triple Spar floater, also of the INNWIND.EU project [1;2]. The purpose of the test campaign was to study the dynamic interaction between the wave-induced platform motion, the aero-dynamic rotor forcing and the control system. Additionally, the tests served to validate the floater design in a number of wave climates with and without wind and to establish a data set for validation of numerical models. As for the first test campaign of

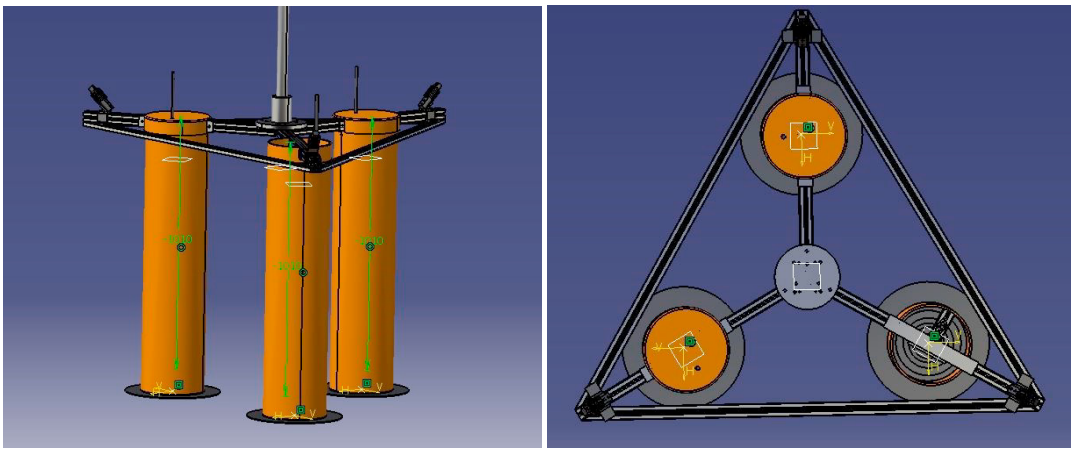

Fig. 1. The geoemetry of the Triple Spar floater at model scale.

the INNWIND.EU project [16], an alternative rotor forcing technique of a ducted fan, see Azcona et al.[17] was also tested. These ducted fan tests, however, are not reported here.

In the following, the Triple Spar floater concept and the experimental setup is described (section 2,3), followed by a brief description of the controller design and implementation (section 4), which is described in full detail in the companion paper of Yu et al [18]. Initial calibration of the wind field and ID tests of the rotor performance is presented in section 5, followed by a set of reference results in section 6. Here, we focus on response to regular waves, and a focused wave group test that illustrates the effect of aerodynamic damping. Measurements of the control-induced platform pitch instability are presented for a wind-only case, followed by a comparison of dynamic response in irregular waves with three different control strategies. Finally, in section 7, results of our first re-modelling results with the FAST model are presented. The paper concludes with a summary in section 8.

2. The Triple Spar Concept

The Triple Spar concept [1;2] is a semi-submerisble platform that supports the DTU 10MW Reference Wind Turbine [14]. The full scale platform consists of three vertical reinforced concrete cylinders that are connected to the wind turbine base through a steel tripod structure. The cylinders are hollow and partially filled with ballasting material to achieve the required draft. The platform is restrained on the sea surface by a three-line catenary mooring system, where each line is connected to one of the cylinders as defined by Borg[19]. Further details on the concept design can be found in [1;2]. The floater has been used also in the LIFES50+ project as example concept for tests of efficient numerical tools for design [20;21]. A FAST setup of the full scale configuration with the DTU 10MW reference turbine is available [2;19].

The Froude scaling law with a geometric scaling ratio of 1:60 was applied for the model tests, following the work of Martin et al.[6], see also Bredmose et al.[22]. The layout of the model-scale floating platform is depicted in Figure 1 and the model-scale floating wind turbine is shown in Figure 2. Table 1 provides the main properties of the system at full and model scale. In the remainder of the paper, and unless specified otherwise, all the properties correspond to model scale.

3. Experimental setup and the model scale turbine

The model tests were carried out at DHI Denmark in a 3 m deep basin, 30 m wide and 20 m long. A top view of the basin and test setup is provided in figure 2, which also shows the placement of the 11 wave gauges applied through the campaign. For initial calibration, tests with no structure in the basin was carried out with a wave gauge placed at the location of the structure. The wave basin is equipped with 60 hinged wave paddles at one of the long sides, enabling generation of uni- and multi-directional sea states as well as focused wave groups and regular waves. A passive wave

Dimension	Prototype Scale	Froude Model Scale	Actual Model Scale (incl. instrumentation)
Platform			
Draft	54.5m	908mm	918mm
Elevation of tower base above MSL	25.0m	417mm	333mm
Column diameter	15.0m	250mm	250mm
Column length	65.0m	1083mm	1100mm
Deck elevation above MSL	10.5m	175mm	182mm
Centre offset from tower centerline	26.3m	438mm	430mm
Tripod overall height	15.0m	250mm	-
Heave plate diameter	22.5m	375mm	375mm
Heave plate thickness	0.5m	8.3mm	3mm
Displaced volume	29224m^3	0.1353m^3	0.1357m^3
Platform mass	28229t	130.69kg	129.35kg
Centre of mass below MSL	36.02m	600mm	646mm
Mooring lines			
Water depth	180m	3.0m	3.0m
Fairlead position above MSL	8.7m	145mm	145mm
Fairlead radius from tower	54.5m	908mm	908mm
Anchor radius from tower	600m	10.0m	10.0m
Chain length	610m	10.17m	10.17m
Tower			
Diameter	7.82m-5.50m	130mm-92mm	80mm
Tower length	95.6m	1594mm	1682mm
Hub height above MSL	119m	1983mm	2070mm
Mass	469t	2.12kg	2.250kg
Nacelle			
Rotor diameter	178.3m	2972mm	2972mm
Blade Length	86.5m	1440mm	1440mm
Blade mass	41.7t	0.188kg	0.198kg
Nacelle+hub mass	552t	2.49kg	2.896kg
Nacelle+hub+rotor mass	677t	3.06kg	3.490kg

Table 1. Key specifications of the prototype scale wind turbine, the ideally Froude scaled 1/60 model, and the actual scaled 1/60 model.

absorber is placed at the down-wave end of the basin, to damp the waves and avoid reflection from the back wall. The turbine was placed 5 m from the wave maker, at the centerline of the basin.

3.1. Mooring system

The mooring system layout is depicted in Figure 2. The mooring system was re-designed to fit within the confines of the wave basin, as detailed by Borg[19]. This re-design did not noticeable affect natural frequencies of vertical degrees of freedom, and the changes in horizontal degrees of freedom were small enough such that the natural frequencies remained significantly separated from the wave excitation frequency range. As part of the design, it was ensured that the chain would not lift completely from the basin floor during operation of the turbine. Steel chain was used that satisfied the Froude-scaled properties of the full-scale mooring lines. Concrete blocks were used as anchors points at the bottom of the basin, and force gauges were installed at the fairlead connection to measure the line tensions.

3.2. Wind generator

The wind was supplied by a 4 m $\times$ 4 m open jet wind generator, built for the previous TLP campaign [12;13]. It consists of six units where a fan blows air laterally into a chamber, where next a set of guide vanes turns the flow 90°

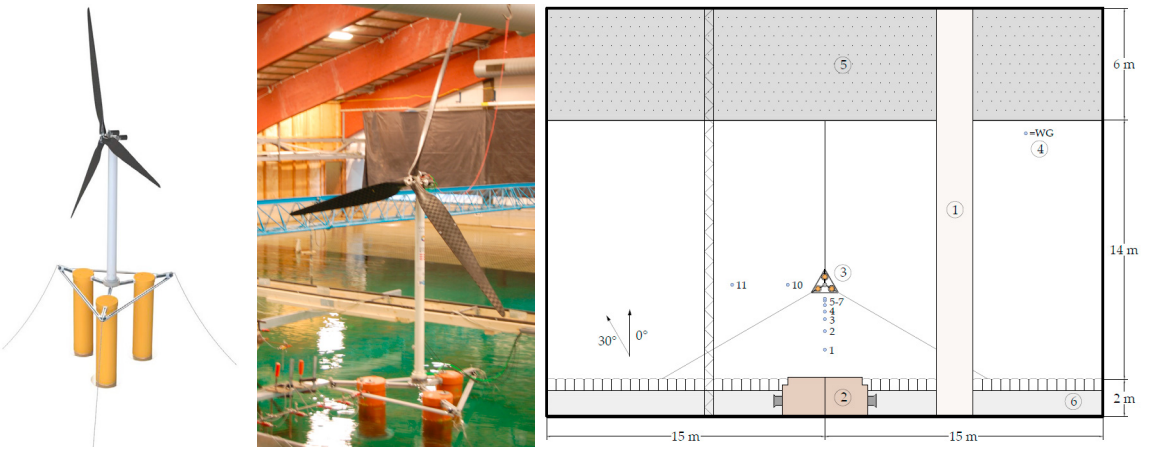

Fig. 2. Left: Scale model visualisation. Middle: Scale model in DHI wave basin. Left: Basin layout. The numbers indicate the wave gauge placements.

to the outflow direction. Two set of screens were mounted at the outlet to straighten the flow. A picture of the system is shown in figure 3.

For the present campaign, new fan motors and steering was mounted to increase the original limit of 1.7 m/s to 2.2 m/s. During the motor replacement, the fan rotors were taken out and put back in. Unfortunately, for the present test campaign, the two upper and mid-left fan rotor were remounted with the rear side facing outward. This led to reduced performance of the affected units and an un-wanted vertical inverse shear of the velocity profile, see section 5. This shear was detected early in the campaign, and partially compensated by adjustment of the individual units fan speeds. The source of the shear, however, was identified at a very late stage in the campaign and it was therefore chosen to fix it only after the tests, to maintain comparability over the full test campaign.

3.3. The model scale turbine

The test turbine and rotor was the same as that used in the TLP campaign, apart from additional stiffening of the nacelle to avoid rocking vibrations of the rotor plane; replacement of the two servo motors for shaft speed and blade pitch by similar JVL units but different steering interface and removal of a gear. As described in Pegalajar Jurado et al.[13] the turbine is a 1:60 Froude scaled model of the DTU 10MW reference. The geometry and mass properties are shown in table 1 where also the full scale values and the ideal Froude scaled target values are provided. Due to the

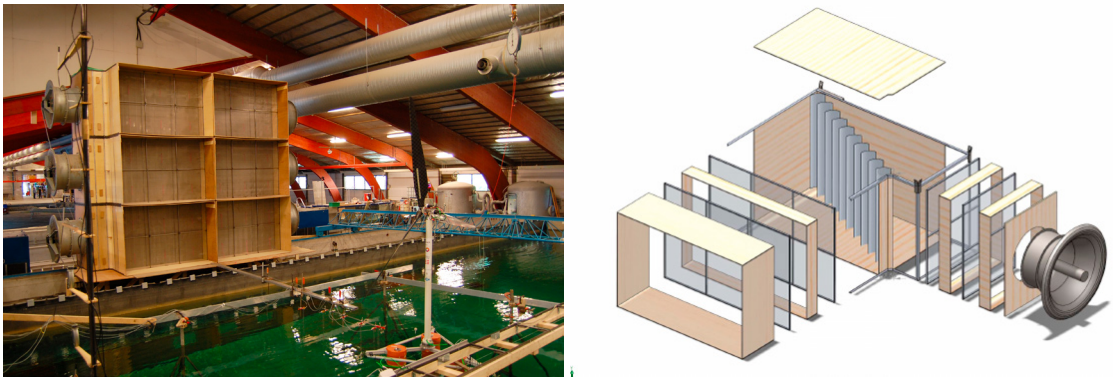

Fig. 3. The wind generator. Left: Turbine in front of the generator. The vertical pole and rail system for wind field calibration are visible in the left and lower regions of the image. Right: Cascaded view of one unit (from Hansen and Laugesen[23]).

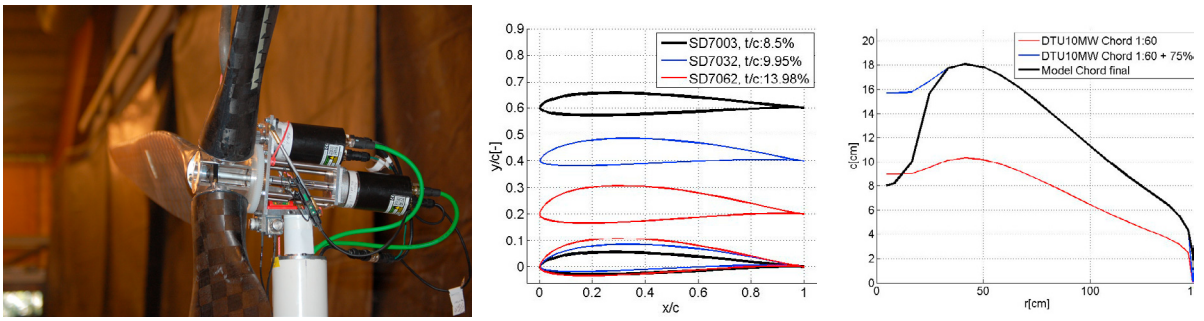

Fig. 4. Left: The turbine nacelle and rotor. Middle: The airfoils and their placement along the blade radius. Right: The chord distribution relative to the full scale blade.

cube-law scaling of mass in Froude scaling, the model scale masses need to be quite small for some elements. The main challenge here is the blade mass and the nacelle+hub mass. For the model scale turbine, the blade mass of 198 g is only 5% larger than the target value. For the nacelle, the removal of a gear lead to a smaller nacelle mass than for the TLP campaign. The nacelle+hub+rotor mass of the present setup was thus 3.49 kg, which represents an over-weight of 14% relative to the Froude scaled target. This extra weight in the nacelle did not lead to any modification in the support structure.

The nacelle was constructed with two JVL MAC050 servo motors which controlled the shaft speed and the collective blade pitch. A picture of the nacelle is shown in figure 4. A gear of ratio of 1:5 was applied between the servo and the shaft. The blade pitch angle was controlled and measured by a fiber-optic gauge.

As already mentioned, the low Reynolds number at model scale necessitates a re-design of the rotor to achieve the right scaled thrust. To this end, the applied rotor design was based on the low Reynolds number Selig Donovan (SD) profiles, supported by 2D wind tunnel measurements of the profile polar at the low Reynolds numbers. To achieve the needed scaled rotor thrust, the chord length was increased by 75% relative to pure geometric scaling of the full scale blade. The profiles and chord distribution are shown in figure 4. Further details of the rotor design can be found in Mikkelsen[15]. The thrust curve shown in Pegalajar Jurado et al.[13] demonstrates that the rotor is able to deliver the target thrust with only minor adjustment of the operational blade pitch angle.

3.4. Instrumentation

The tests were logged at 160 Hz by DHIs data logging system. The following data were logged

- Up to 11 wave gauges placed at the center line of the basin and with two gauges placed laterally offset from the turbine
- The inline and lateral shear force between the nacelle and tower top
- The inline and transverse acceleration in the nacelle
- The inline and transverse acceleration in the floater
- The six degree of freedom floater motion, measured with a Qualisys Motion Track system
- The mooring line tension, measured at the connection between mooring cable and floater
- The instantaneous position of one wave flap
- The rotor speed
- The blade pitch angle
- The torque of the shaft servomotor

Initially, the rotor speed was logged directly from the motor. However, as the binary protocol used for this was very limited in resolution, a work-around was implemented through instantaneous differentiation of the low-pass filtered azimuthal shaft angle. This provided a much smoother output.

4. Control system

A central part of the test campaign was the inclusion of real time blade pitch control. Five controllers were designed and tested, along with tests for fixed blade pitch. The controller design, hardware implementation and detailed analysis of controller-specific tests are reported in the companion paper of Yu et al.[18], see also Yu[24]; Lomholt and Boehm[25]. We here summarize the key points. The control strategy follows that of the DTU 10 MW reference wind turbine. The input to the controller is the instantaneous shaft speed and the actual blade pitch angle. Figure 5 shows the control regions in terms of rotational speed and generator torque. Below rated wind speed at 1.47 m/s, optimum C_P tracking is achieved through torque control

$$\tau_{\text{gen}} = K\Omega^2 \tag{1}$$

and the blade pitch is kept fixed. Here τ_{gen} is the generator torque, Ω is the shaft speed and K is a control-specific constant. Above rated wind speed, the generator maintains a constant torque while the rotor speed is controlled by PI control of the blade pitch angle

$$\Delta\theta = K_P\Delta\Omega + K_I \int_{t=0}^{\infty} \Delta\Omega \, \mathrm{d}t. \tag{2}$$

where θ is the blade pitch angle and $\Delta\Omega = \Omega - \Omega_{\text{rated}}$. As described by Larsen and Hanson[26], see also [27–29], the values of K_P and K_I governs the time scale of the controller action. By insertion of (2) into the drive train equation of motion, one may obtain an autonomous second-order ODE for the instantaneous shaft angle. The ODE has two complex conjugate eigen solutions which characterizes the natural frequency ω_Ω and damping of the coupled shaft speed and controlled blade pitch.

Special settings for floating wind turbines are needed due to the small natural frequencies of the floater pitch motion ω_{pitch}. The problem was first described by Larsen and Hanson[26] in relation to the HyWind project. During a motion cycle at the platform pitch frequency, the rotor will experience a stronger wind speed as it moves into the wind. For wind speeds larger than rated, the standard control action will be to pitch the blades into the wind to reduce the aerodynamic torque. Hereby also the thrust is reduced, corresponding to an added force in the direction of motion. At the second half cycle of platform pitch motion, where the rotor moves along with the wind, the apparent wind speed is reduced and the standard control action will reduce the blade pitch to increase the torque. Again the associated thrust

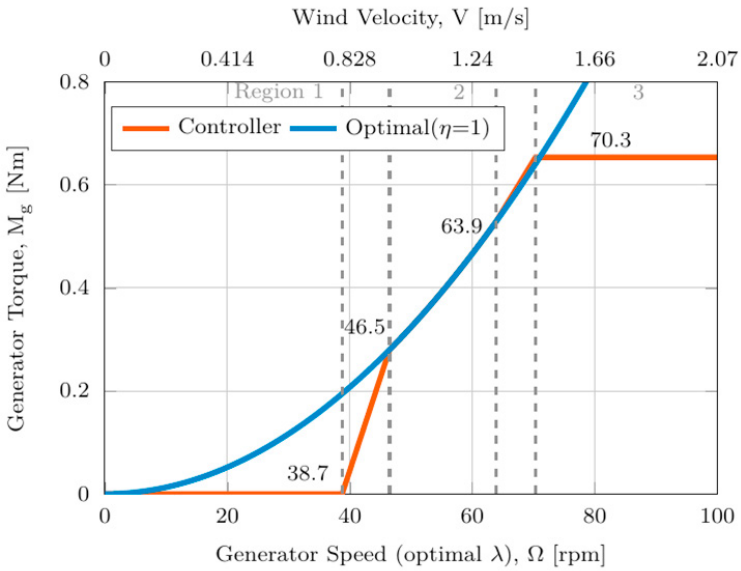

Fig. 5. Control strategy for the turbine at model scale.

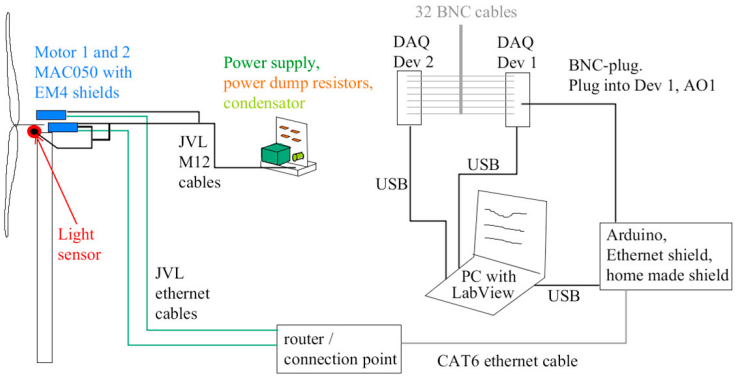

Fig. 6. Sketch of the hardware setup.

change will be in the direction of the motion and a net work is thus exerted during a platform pitch cycle. A similar mechanism would also be possible for the surge mode, but often the viscous hydrodynamic damping of the floater for this mode results in a net positive damping and thereby eliminates the instability.

While, in principle, this phenomenon could also occur for a bottom-fixed turbine, the first natural frequency of tower fore-aft motion is too large for the control system (and most likely also the aerodynamic inflow) to follow and excite the instability. For the floating turbine, however, the natural frequency of the controller is larger than the platform pitch frequency and the instability can occur.

A simple solution to get around the instability is therefore to reduce the natural frequency of the controller by modification of K_P and K_I [26]. While the five tested controllers are described in detail in Yu et al.[18], we here report results of two controllers plus fixed blade pitch

C1.0 Land-based controller with $\omega_\Omega = 1.1\omega_{\text{pitch}}$

C4.3 Tuned controller with $\omega_\Omega = 0.7\omega_{\text{pitch}}$

Fixed blade pitch The blade pitch is fixed according to the mean wind speed. The shaft servomotor regulates towards rated speed. We will denote this controller as the 'fixed' controller for short in the following

Here C1.0 is designed to demonstrate the effects of the instability, C4.3 is designed to yield stable operation and 'fixed blade pitch' is designed to show the effect of fixed blade pitch and fixed rotational speed. The latter is obtained through torque control of the shaft servo motor. The hardware implementation of the control is sketched in figure 6. The shaft speed and blade pitch servo motors were connected through Ethernet cables to an Arduino MEGA ADK micro controller, and a communication via the Modbus protocol was established. The micro-controller was further interfaced by a Lab View setup at a laptop, that also transferred the data of blade pitch, shaft speed, and generator torque to the data acquisition system.

5. Initial tests and calibration

Before the production tests, several calibration tests were carried out. A number of wave calibration tests with an empty basin was made to measure the ambient wave fields for the case of no structure, also at the position of turbine installation. Next, the wind field was measured by traversing a hot wire wind gauge at the downwind distance of 5 m from the 4×4 m^2 outlet area of the wind generator. Four hot wire probes were mounted on a vertical pole that was moved continuously at a rail-cart system in the horizontal direction. By repeating three times, measurements at 12 horizontal lines of different vertical level were obtained. This allowed adjustment of the fan speed for the wind generators.

The measured vertical wind profiles are shown in figure 7. The inverse vertical shear, caused by the reversed fan-blade mounting as discussed in Section 3 is evident and can be seen to increase with increasing wind speed. In this plot, the 4 m vertical extent of the wind generator area is marked by horizontal dashed lines. The rotor spans 1.5 m to

each side of the hub-level, indicated by a solid line. It can thus be seen that the lower part of the rotor swept area is below the extent of the wind generator, although the open jet flow will most likely spread to this region too over the 5 m distance from the outlet to the turbine. Measurements in later campaigns indicate that this is true at rated wind speed (1.47 m/s), while at e.g. 2 m/s the velocity in this region can be reduced to about 80% of the target value. The turbulence intensity measured in the rotor area was of magnitude 10% at rated wind speed and of 15-20% magnitude for the largest wind speed. No quantification of the spatial coherence was made. During the tests with the floating structure in the basin, the mean wind speed for each test was set by knowing the corresponding fan speed with no additional measurement of the wind field.

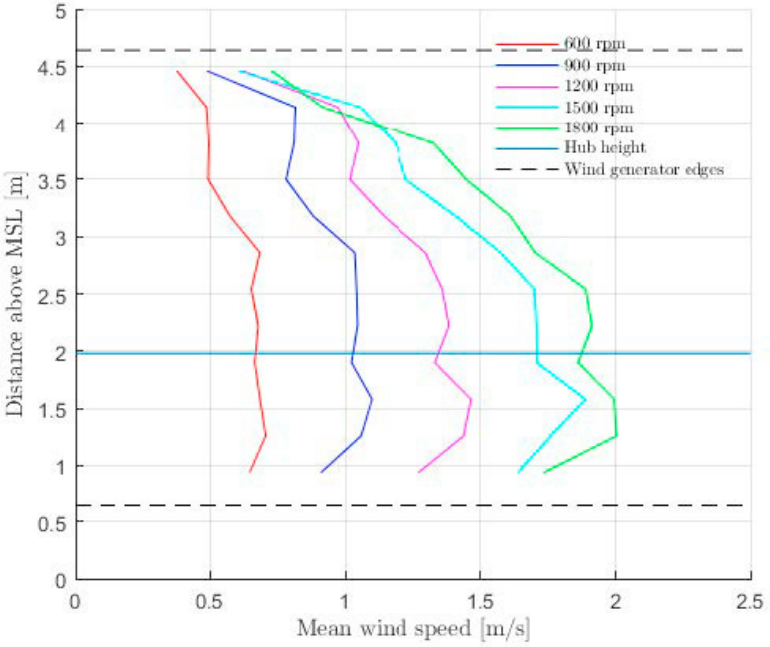

Fig. 7. The measured wind profiles at different target wind speeds.

After the wind field calibration, rotor ID tests were carried out to establish the operational settings of the rotor and control system. An example of such a rotor ID test and post processing is shown in figure 8 at 1.6 m/s. At a fixed wind speed, and fixed blade pitch, the shaft servo motor was set to maintain the Froude scaled rotor speed for that specific wind speed. The generator torque needed to maintain the target rotor speed at the given wind speed was noted down together with the corresponding thrust. Next, the blade pitch was changed, and the corresponding new values of torque and thrust identified. The tests were carried out for five blade pitch angles ($\theta_{\text{target}} + \{-2, -1, 0, 1, 2\}^\circ$) and five wind speeds. Hereby, the target operational values of the blade pitch that yields the correct scaled thrust was identified. Further, the control parameter K for the torque controller below rated speed was identified along with the torque to apply for shaft speeds at and above the rated shaft speed. While these values had already been determined numerically in the controller design, the present method eliminates the errors from unknown frictional losses and in-accuracies in the aerodynamic modelling.

5.1. Natural frequencies

The natural frequencies of the floating turbine configuration was identified through decay tests. Table 2 summarizes the results. The upper limit of the 3P forcing frequency has been included as well, to ease interpretation of power spectral plots.

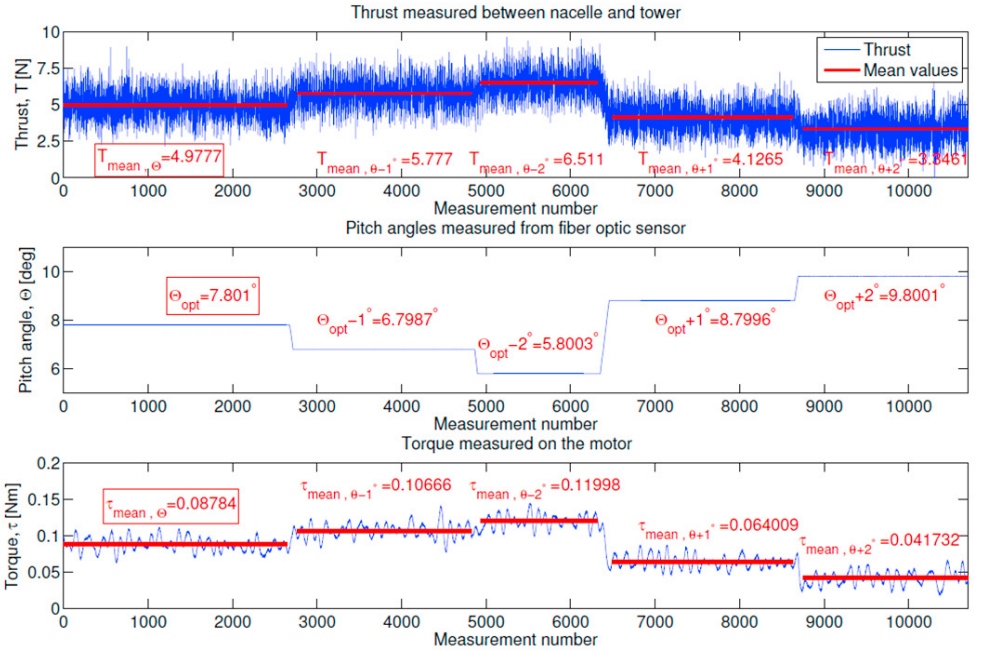

Fig. 8. Analysis of a rotor ID test at a wind speed of 1.6 m/s.

Mode	Frequency [Hz]
Surge	0.05
Pitch	0.28
Heave	0.47
Tower	3.3
3P, rated	3.7

Table 2. Natural frequencies in lab scale for the floating turbine in moored condition. The 3P frequency at rated wind speed (upper nominal limit) is shown too.

	Model scale			Full scale		
Sea state	H_s [m]	T_p [m]	V [m/s]	H_s [m]	T_p [m]	V [m/s]
1	0.039	0.71	0.9	2.36	5.50	7.00
2	0.048	0.78	1.0	2.85	6.04	7.80
3	0.055	0.84	1.1	3.31	6.50	8.50
4	0.062	0.89	1.3	3.71	6.89	10.1
5	0.069	0.94	1.5	4.14	7.28	11.6
6	0.080	1.01	1.7	4.78	7.82	13.2
7	0.091	1.08	1.9	5.46	8.37	14.7
8	0.129	1.29	1.9	7.74	10.0	14.7
9	0.159	1.43	1.9	9.54	11.1	14.7
10	0.200	1.60	1.9	12.0	12.4	14.7

Table 3. The sea states and corresponding wind speeds as tested in the lab.

6. Results

The wind turbine configuration was tested in a range of wind-wave conditions and with different control strategies. The full set of wind-wave climates are shown in table 3, where state 1-5 have identical parameters to climates 1-5 of the DTU TLP campaign [13]. Sea state 6 and 7 were new for the present campaign and included to have test conditions above rated wind speed at 1.47 m/s, where control region 3 is active. Further, sea state 8 is identical wave-wise to sea

state 7 of the TLP campaign. For sea states 7-10, the wind speed was limited by the maximum value of 1.9 m/s for the present setup.

The wave conditions tested include regular waves, focused wave groups and irregular waves. Some climates were also tested with a 30° mis-alignment of the wave direction relative to the wind direction. This was achieved by turning the wave field 30° using the directional wave maker. The tests with active control were mainly carried out for sea states 3, 5, 6 and 7.

The surface elevation reported in following plots was measured by a wave gauge located on the side of the floating platform (wave gauge 11 in 2, right). Given the short distance of 5m from the wave maker to the floater, it was assumed that the wind field did not affect the waves.

6.1. Regular waves

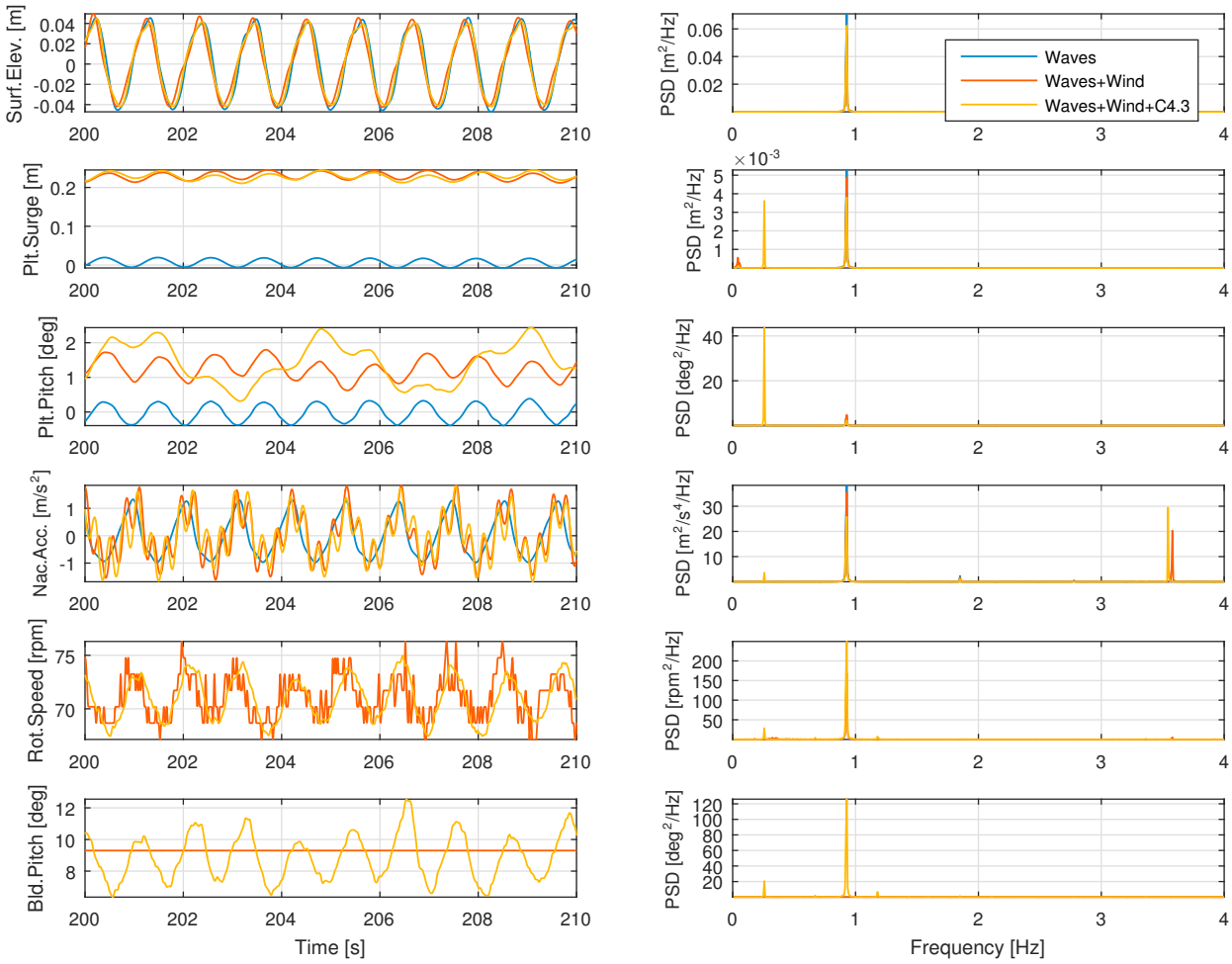

Fig. 9. Response for regular wave forcing (sea state 7). Left column shows time series and right column shows power spectra.

We first report on results for regular waves of sea state 7. Time series and power spectra for free surface elevation, platform surge, platform pitch, inline nacelle acceleration, rotor speed and blade pitch are shown in figure 9. The plots include results of wave-only tests (blue), waves+wind with fixed blade pitch (red) and waves+wind with the tuned C4.3 controller (yellow). Additionally to the change of equilibrium position from the mean thrust, the turbulence in the wind field and and the change of inflow caused by the platform motion introduce dynamic effects. The basic test condition of regular waves allows interpretation of the different control strategies and their effects on the resulting

motion. For the case without control, the blade pitch was set to the value that gives the correct mean thrust at the given wind speed. The time series in the plots are restricted to an interval of 10 s to allow clear reading of the signals. The power spectra, however, are based on the full test duration of 240 s (lab time), with exclusion of initial transients.

For the platform surge motion, the presence of wind leads to a notable offset and introduces spectral energy at both the platform surge and pitch natural frequencies, additionally to the wave frequency. A similar offset can be seen in the platform pitch signal, where for the case of active blade pitch control, motion at the platform pitch frequency is evident both in the time series and in the power spectra. Also for the fixed blade pitch control, energy at the platform pitch frequency is observable, but to a smaller extent. Both observations agree with the expectation: although controller C4.3 is 'slowed down' to avoid the platform pitch instability, the presence of active blade pitching will still lead to reduced effective damping at this mode. Hence, any wind-driven forcing of this mode will be amplified by the presence of the natural mode, and the damping will be less for the C4.3 controller than for the fixed blade pitch control.

The rotor speed fluctuations are mainly taking place at the wave frequency, where both controllers follow the wave-induced velocities. The reason for the fixed controller to show fluctuations of rotor speed is due to a low strength of the torque control applied by the servo motor. With the chosen gear ratio of 1:5, the motor was operated close to its torque limit, thus leaving only limited reserves for the torque control. Both controllers thus operate to maintain a constant shaft speed, the fixed one through the generator torque and the tuned one through a changed blade pitch. The latter strategy is associated with changes in aerodynamic thrust, which in the present case leads to enhanced motion at the platform pitch frequency. Further, the limited resolution of the speed output, as described in section 3.4 is visible through the 1.5 rpm jumps of the signal for fixed control.

The blade pitch signal of the blade-pitching controller shows a similar behaviour as the rotor speed with main fluctuations at the wave frequency and some presence of motion at the platform pitch frequency. For all three tests, the nacelle accelerations are similar and dominated by motion at the 3P frequency. As shown in table 2, this frequency is not far from the tower fore-aft frequency and notable response is seen. It should also be noted that due to the 75% increase in blade chord, the shadow effect from the tower is likely to be stronger than would be the case for the proto-type scale turbine.

6.2. Focused wave group impact

We next discuss results for a focused wave group event, produced as a New Wave group for sea state 7 [30–32] with linear target wave height of $1.86 \times H_s$. Time series and power spectra are shown in figure 10, this time for waves-only and fixed control.

The purpose of the comparison is mainly to demonstrate the effect of wind when added to the wave forcing. For both the platform surge and pitch signals, the offsets from the presence of wind are clearly visible. The wave group forces motion at its fundamental frequency range around 1 Hz and next excites substantial motion at the natural surge and pitch frequencies. While the surge motion time series seems quite un-affected by the presence of wind, except for the offset, the platform pitch motion shows substantially stronger damping from the wind. This is a clear manifestation of aerodynamic damping, which can also be observed in standard decay tests in calm water with and without wind. The aero-dynamic damping is also evident in the power spectrum, which shows that the wind acts to damp both the natural surge and pitch motion. The damping of surge motion is smaller, though. This can be explained by the smaller frequency and the missing amplification of nacelle motion relative to floater motion for this mode.

For the nacelle acceleration, the present results do not allow a discussion of the damping effects at the dominating 3P motion, since this is not present for the wave-only case. The damping of the platform pitch motion, however, is still evident at the natural pitch frequency. Further, still for the case with wind, the nacelle acceleration shows a small amount of spectral energy at the tower frequency, just below the 3P frequency.

6.3. Platform pitch instability

A central aim of the present campaign was the quantification and insight into the dynamic interaction with the controller, including the instability effect discussed in section 4. Some presence of the instability was seen for regular waves. An isolated demonstration of the effect, however, is provided in figure 11 where the C1.0 ('land based') and C4.3 ('tuned') controllers are compared at calm water at the wind climate of sea state 6.

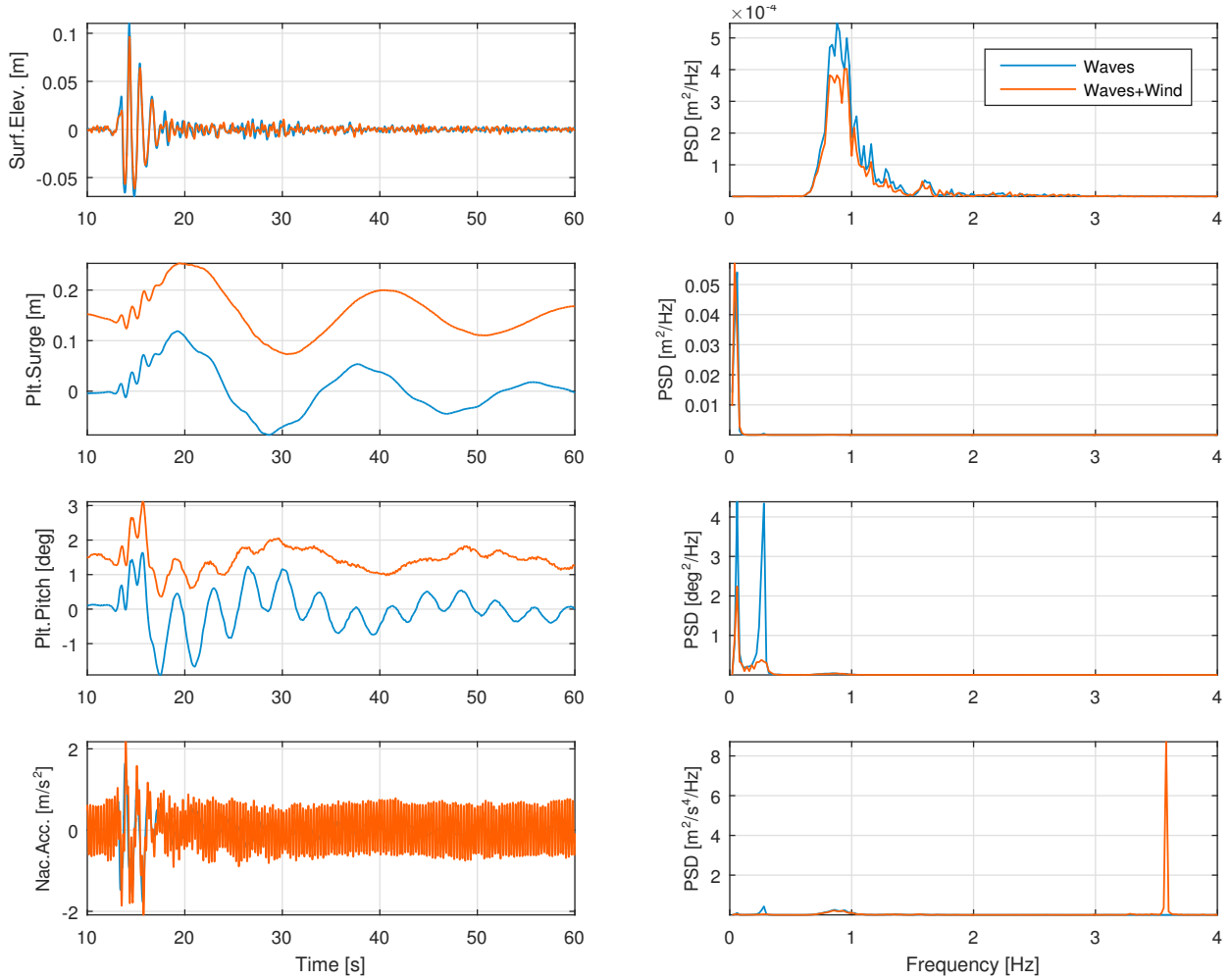

Fig. 10. Response for a focused wave group impact of sea state 7 with and without wind. Time series and power spectra.

The tests with the land-based controller shows a clear growth of the instability at the platform pitch frequency for all signals. The blade pitch motion and rotor speed follows the structural motion. The nacelle acceleration show energy at the 3P frequency for both signals. The plots, though, gives clear evidence of the existence of the instability, as has also been reported by Karikomi et al.[8].

6.4. Irregular waves

Since the instability has now been observed in isolated form and under regular wave motion, a central question is now how big a role it plays for a real sea state where both the wind and waves are stochastic. To this end, we report results from sea state 7 in aligned conditions with the fixed, land-based and tuned controller. Time series and power spectra are shown in figure 12

For all three control strategies, the surge response is dominated by motion at the natural surge frequency, overlaid by wave forcing.

The platform pitch motion show strong energy content at the platform pitch frequency, most pronounced for the land-based controller and least pronounced for the fixed controller. This is in line with the expectation, that the land-based controller has negative effective damping at the platform pitch mode, and the tuned controller reduced damping, relative to the most damped fixed control strategy. For the two blade-pitching controllers, the blade pitch and rotor

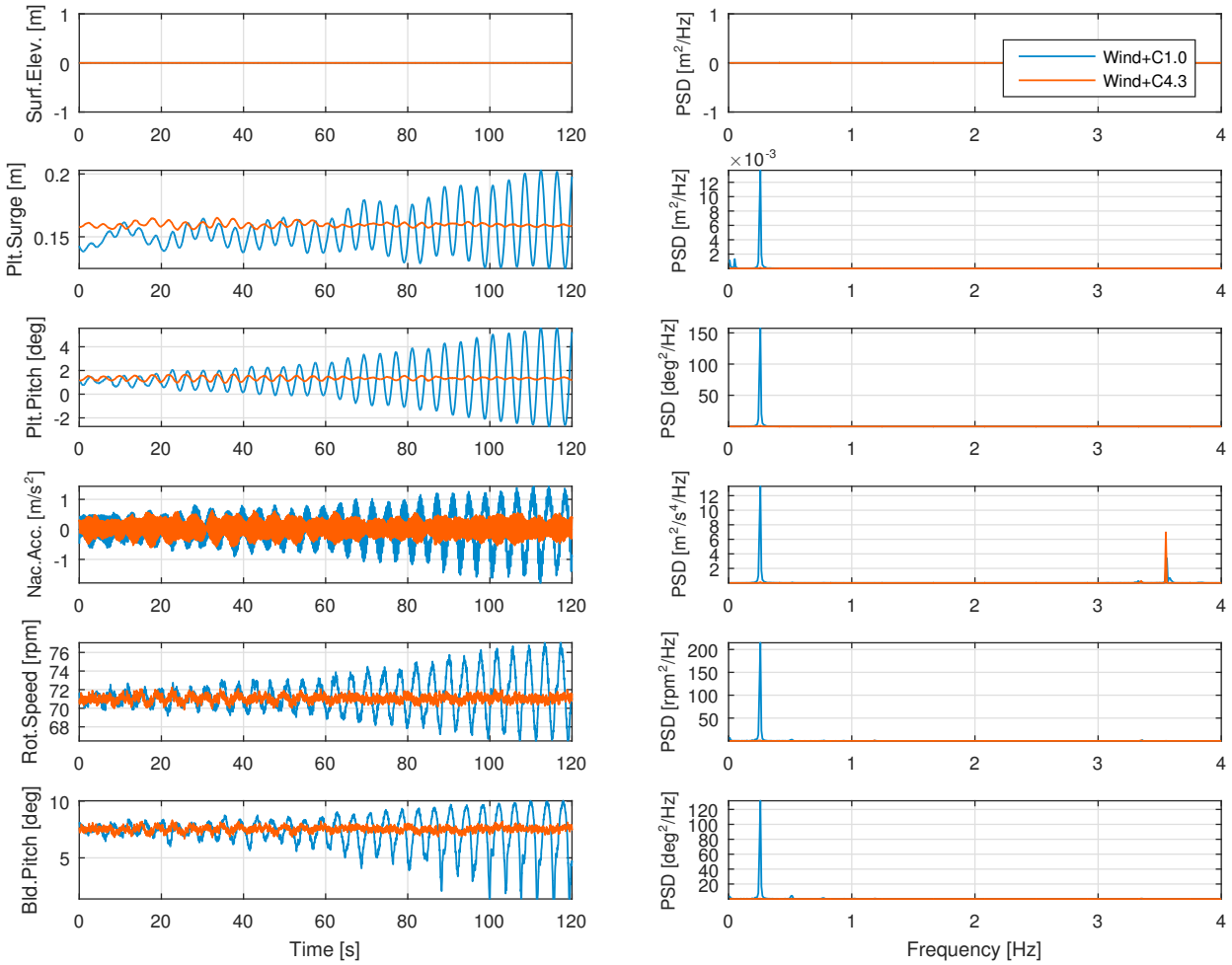

Fig. 11. Demonstration of the platform pitch instability in wind only conditions. Land-based and tuned controller. Wind speed is 1.7 m/s (13.2 m/s full scale).

speed fluctuations shows motion at both the lower end of the wave spectrum and at the platform pitch frequency. For all three tests, the nacelle acceleration is dominated by 3P motion.

The extent of the motion response is further analyzed through exceedance probability plots, as shown in figure 13 for free surface elevation, platform surge and pitch, nacelle acceleration, rotor speed and blade pitch angle. Exceedance probability plots can be made with different methods for peak selection. For the present analysis, the plots were made 'per wave' by taking one response peak for each wave, based on the free surface elevation signal.

Both the platform surge and pitch show the largest motion for the land-based controller, smaller motion for the tuned controller and smallest motion for the fixed controller. This is in agreement with the findings at time series level and can be explained by the increasing amount of damping for this controller sequence.

The nacelle accelerations are much more in agreement for the three controllers. This is very likely due to the dominance of motion at the 3P frequency, which is too large for interaction with the rotor dynamics. For exceedance probabilities above 6%, however, the accelerations show the same ordering as for the platform motion, i.e. largest response for the land-based controller, followed by the tuned and next the fixed controller. This is a likely footprint of the platform motion on the tower response. For the extreme events, the response of the fixed control strategy are seen to be largest and smallest for the tuned controller.

The rotor speed fluctuations are smallest for the tuned controller. This may be explained by noting that this controller is designed to yield stable motion and some regulation of the aerodynamic forcing to achieve a constant

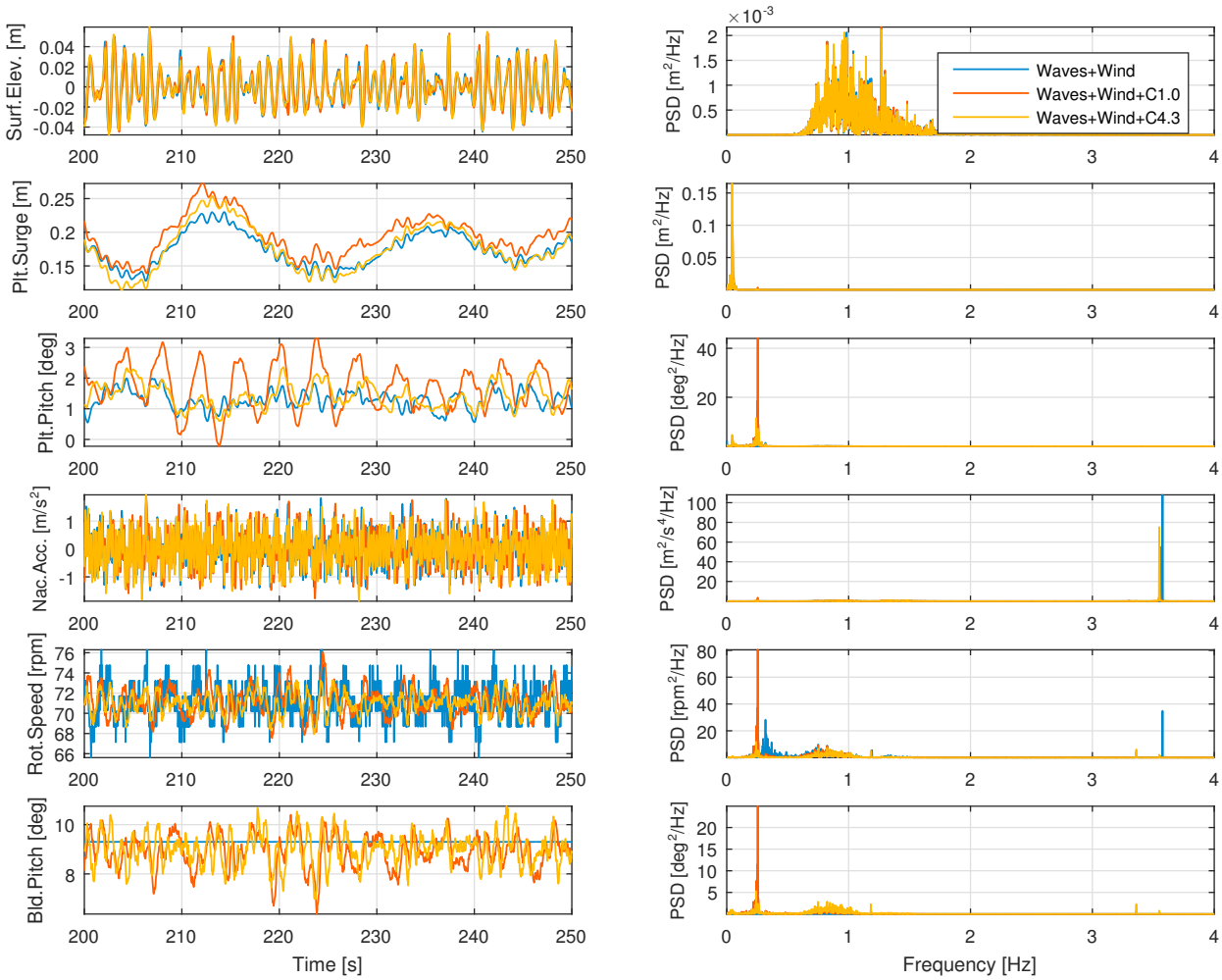

Fig. 12. Response to irregular waves and wind forcing under fixed blade pitch, land-based and tuned control. Time series and power spectra.

rotor speed. The fixed controller gives larger fluctuations due to the weaker torque control offered by the servo motor on the shaft. Conversely, the land-based controller is able to operate more aggressively with the blade pitch, which in turn excites pronounced fluctuations at the platform pitch frequency and thus an increased fluctuation level for the rotor speed.

For the blade pitch angles, the tuned controller is seen to have larger fluctuations than the land-based. This can be explained through the faster reaction time of the land-based controller, which is thus able to control the shaft speed with smaller blade-pitch action than the tuned controller which has been slowed down to avoid the platform pitch instability.

7. First results of re-modelling

A FAST Jonkman and Jonkman[33] model has been set up, based on WAMIT computation of the hydrodynamic platform properties and the MoorDyn module. The model was tuned against decay tests for the clamped tower and platform surge and pitch decay tests for the full turbine configuration.

A first comparison for a wave-only test for regular waves of sea state 7 are shown in figure 14. The measured signal from wave gauge 10 was used as input to the model.

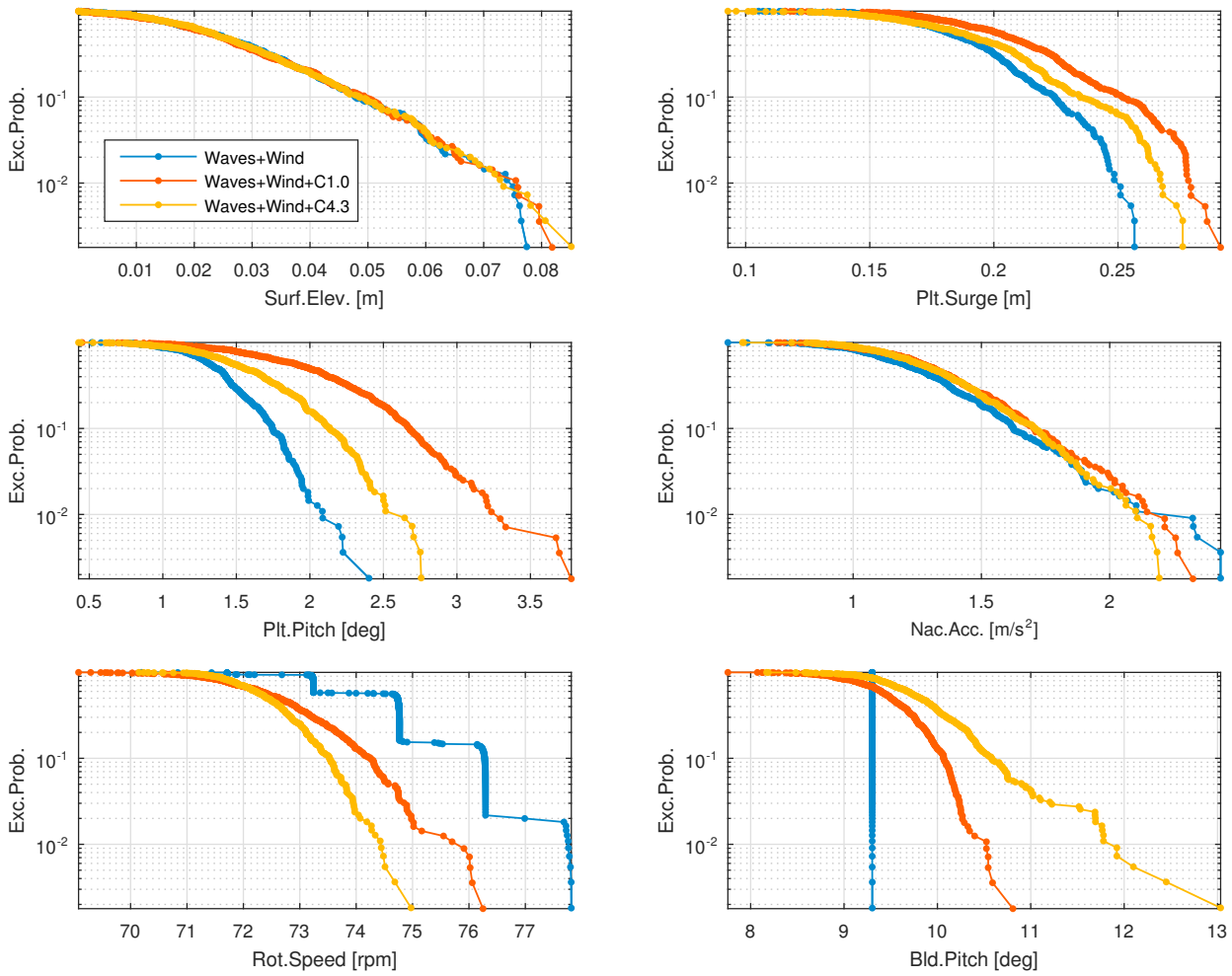

Fig. 13. Response to irregular waves and wind forcing. Exceedance probability plots (one peak per wave) of platform, nacelle and rotor motion.

The results are generally in good agreement, with a slight under-prediction of the surge motion amplitude. The measurements also show some motion at the platform modes, which is likely to be a transient and therefore not picked up by the model. The heave motion of the tests is of quite small amplitude, less than 1 mm, and therefore contain some background noise. Nevertheless, the model agreement at the wave frequency and the natural heave frequency is good. The test results further show some heave response at twice the wave frequency. This is the set-down effect induced by the mooring system, that under the positive and negative surge half-cycles provide an increased downward force. The results for the platform pitch and nacelle acceleration show a very good match to the test results. Further re-modelling of irregular sea states and combined wind and wave forcing is subject to current research.

8. Summary and conclusions

A setup for a test campaign with the Triple Spar floater and the DTU 10MW reference wind turbine has been described. The purpose of the tests was to quantify the effects of wind and wave force interaction through the structural response and the interaction with the blade pitch controller. Results have been presented for a fixed blade pitch control strategy, a land-based controller and a tuned controller in terms of time series, power spectra and exceedance probability plots.

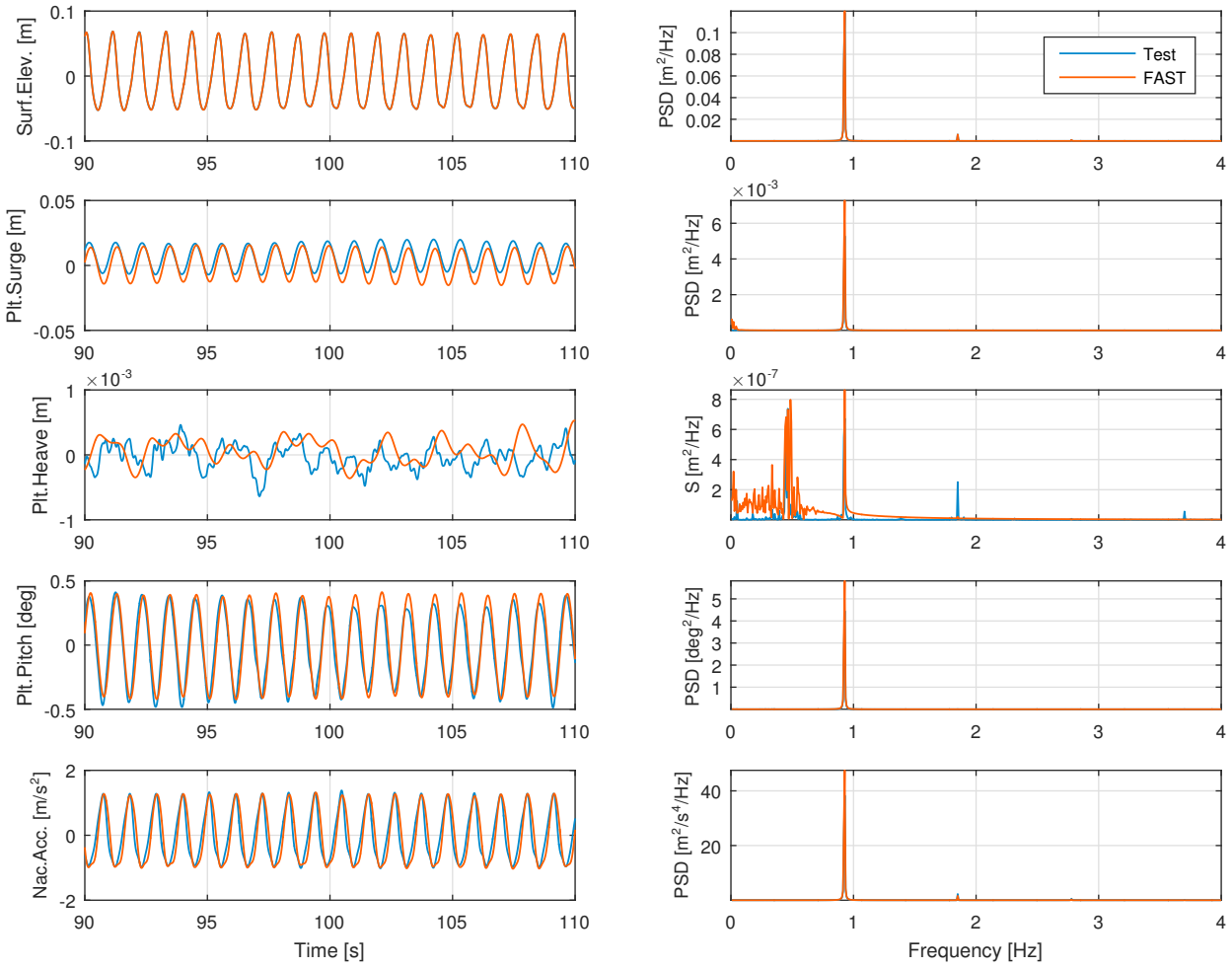

Fig. 14. Re-modelling of a wave-only test in FAST for regular waves (sea state 7). Time series and power spectra of response.

From the tests of regular and focused wave group forcing, the steady offset in platform surge and pitch due to the steady mean thrust force was evident. Aerodynamic damping was clearly visible for the decay of the wave group induced motion at the platform pitch natural frequency. A central aim for the campaign was to investigate the instability of motion at the natural platform pitch frequency, associated with too agressive blade pitch control above rated wind speed. A clear measurement of this instability has been presented for a case of wind forcing and no waves. Here, the platform response signals of surge and pitch were seen to build up a cyclic motion at the natural pitch frequency of increasing amplitude, supported by similar variations in rotor speed and platform pitch. Hence, with the present tests, we were able to confirm the numerical prediction of Larsen and Hanson[26] and extend the experimental results of Karikomi et al.[8].

The response of surge, pitch, rotor speed, blade pitch and nacelle acceleration for cases of irregular wave forcing have been analysed with emphasis on the wind- and control-induced effects above rated wind speed. For the wind-wave climate analysed, the platform surge motion was dominated by motion at the natural surge frequency. The response of both platform surge and pitch was found to be smallest for the fixed blade pitch control, with increased response for the tuned controller and largest response for the land-based controller. This was explained by the similar differences in thrust variation for the three control strategies.

The ordering after magnitude for rotor speed and blade pitch variation, however, were found to be different. For rotor speed, the tuned controller showed the smallest variation. Taking that as a base case, both the fixed blade pitch and the land-based controller showed larger variation due to the relatively weak torque forcing of the generator for

fixed blade pitch and the onset of the platform pitch instability for land-based control, respectively. For the two blade-pitching controllers, the variation of blade pitch was strongest for the tuned controller. This was explained through its more slow reaction time, which necessitates a stronger variation for the control to be effective.

The nacelle acceleration was found to be less influenced by the control than the platform pitch motion. This is due to the dominance of nacelle acceleration at the 3P frequency, which for the present tests was relatively close to the first tower fore-aft frequency. For the extreme events of the analysed sea state, the tuned controller was found to give the smallest accelerations, while fixed blade pitch gave the largest. For the main part of the test, however, the largest response of nacelle acceleration was seen for the land-based controller, consistent with the magnitude of platform motion.

Results for re-modelling of the tests with FAST for a waves-only case of regular waves have been presented. The results were generally found to show a good match both for the platform motion and the nacelle acceleration. This is encouraging and motivates further modelling for irregular sea states and simultaneous wind forcing. This is part of present research along with extended analysis of the full data set. The associated insight will contribute to improved understanding and modelling of the interaction effects of wind forcing, wave forcing and control and thereby support improved design of future offshore floating wind turbines.

Acknowledgements

Bjarne Jensen and Jesper Fuchs, DHI Denmark are thanked for their help during the test campaign. JVL Servomotors is acknowledged for assistance in adapting the servo motors into the turbine setup.

References

[1] Sandner, F., Yu, W., Matha, D., Azcona, J., Mundate, X., Grela, E., et al. INNWIND.EU D4.33: Innovative concepts for floating structures. Tech. Rep.; University of Stuttgart; 2014.

[2] Lemmer, F., Amann, F., Raach, S., Schlipf, D.. Definition of the SWE Triple Spar platform for the DTU 10MW reference turbine. Tech. Rep.; University of Stuttgart; 2016. Retrieved July 21, 2016, from http://www.ifb.uni-stuttgart.de/windenergie/downloads.

[3] Skaare, B., Hanson, T.D., Nielsen, F.G., Yttervik, R., Hansen, A.M., Thomsen, K., et al. Integrated dynamic analysis of floating offshore wind turbines. In: Proc. Eur. Wind Energy Conf. and Exhib. (EWEC). Milan, Italy; 2007,.

[4] Nielsen, F.G., Hanson, T.D., Skaare, B.. Integrated dynamic analysis of floating offshore wind turbines. Proceedings of the International Conference on Offshore Mechanics and Arctic Engineering - Omae 2006;2006. doi:10.1115/OMAE2006-92291.

[5] Goupee, A.J., Koo, B.J., Kimball, R.W., Lambrakos, K.F., Dagher, H.J.. Experimental comparison of three floating wind turbine concepts. Journal of Offshore Mechanics and Arctic Engineering 2014;136(2):020906. doi:10.1115/1.4025804.

[6] Martin, H.R., Kimball, R.W., Viselli, A.M., Goupee, A.J.. Methodology for wind/wave basin testing of floating offshore wind turbines. Journal of Offshore Mechanics and Arctic Engineering 2014;136(2):020905. doi:10.1115/1.4025030.

[7] Kimball, R., Goupee, A.J., Fowler, M.J., de Ridder, E.J., Helder, J.. Wind/wave basin verification of a performance-matched scale-model wind turbine on a floating offshore wind turbine platform. 33rd International Conference on Ocean, Offshore and Arctic Engineering, 2014, Vol 9b 2014;.

[8] Karikomi, K., Ohta, M., Nakamura, A., Iwasaki, S., Hayashi, Y., Honda, A.. Wind tunnel testing on negative-damped responses of a 7mw floating offshore wind turbine. Poster presented at EWEA Offshore 2015, Copenhagen; 2015.

[9] Goupee, A.J., Kimball, R.W., Dagher, H.J.. Experimental observations of active blade pitch and generator control influence on floating wind turbine response. Renewable Energy 2017;104:9–19. doi:10.1016/j.renene.2016.11.062.

[10] Savenije, F.. Model testing of a floating wind turbine including control. Presentation at the EERA DeepWind 2017 Conference, Trondheim, Norway. Available at https://www.sintef.no/globalassets/project/eera-deepwind2017/presentasjoner/g1_savenije.pdf; 2017.

[11] Hansen, A., Laugesen, R., Bredmose, H., Mikkelsen, R., Psichogios, N.. Small scale experimental study of the dynamic response of a tension leg platform wind turbine. Journal of Renewable and Sustainable Energy 2014;6(5):053108. doi:10.1063/1.4896602.

[12] Bredmose, H., Mikkelsen, R., Hansen, A., Laugesen, R., Heilskov, N., Jensen, B., et al. Experimental study of the DTU 10MW wind turbine on a TLP floater in waves and wind. Presented at the EWEA Offshore 2015 conference. Available online; 2015.

[13] Pegalajar Jurado, A.M., Hansen, A.M., Laugesen, R., Mikkelsen, R.F., Borg, M., Kim, T., et al. Experimental and numerical study of a 10MW TLP wind turbine in waves and wind. Journal of Physics: Conference Series (online) 2016;753:092007 (11 pp.), 092007 (11 pp.). doi:10.1088/1742-6596/753/9/092007.

[14] Bak, C., Zahle, F., Bitsche, R., Kim, T., Yde, A., Henriksen, L.C., et al. Description of the DTU 10MW reference wind turbine. Tech. Rep. DTU Wind Energy Report-I-0092; DTU Wind Energy; 2013.

[15] Mikkelsen, R.. The DTU 10MW 1:60 model scale wind turbine blade. Tech. Rep.; DTU Wind Energy; 2015.

[16] Sandner, F., Amann, F., Matha, D., Azcona, J., Munduate, X., Bottasso, C.L., et al. Model building and scaled testing of 5MW and 10MW semi-submersible floating wind turbines. Presentation at the 12th Deep Sea Offshore Wind R& D Conference, EERA DeepWind 2015. Available at http://www.sintef.no/globalassets/project/eera-deepwind-2015/presentations/e/e2_sandner_univ-stuttgart.pdf; 2015.
[17] Azcona, J., Bouchotrouch, F., Gonzalez, M., Garciandia, J., Munduate, X., Kelberlau, F., et al. Aerodynamic thrust modelling in wave tank tests of offshore floating wind turbines using a ducted fan. Journal of Physics Conference Series 2014;524(1):012089. doi:10.1088/1742-6596/524/1/012089.
[18] Yu, W., Lemmer, F., Bredmose, H., Borg, M., Pegalajar-Jurado, A., Mikkelsen, R.F., et al. The triple spar campaign: Implementation and test of a blade pitch controller on a scaled floating wind turbine model. To appear in Energy Procedia 2017;.
[19] Borg, M.. Mooring system analysis and recommendations for the innwind.eu triple spar concept. Tech. Rep.; DTU Wind Energy; Kgs. Lyngby, Denmark; 2016. DTU Wind Enery Report-I-0448.
[20] Borg, M., Mirzaei, M., Bredmose, H.. D1.2 wind turbine models for the design. Tech. Rep.; DTU Wind Energy; 2015. Deliverable of the LIFES50+ project.
[21] Lemmer, F., Mller, K., Yu, W., Faerron-Guzman, R., Kretschmer, M.. D4.3: Optimization framework and methodology for optimized floater design. Tech. Rep.; University of Stuttgart; 2016. Deliverable of the LIFES50+ project.
[22] Bredmose, H., Larsen, S., Matha, D., Rettenmeier, A., Marino, E., Saettran, L.. Collation of offshore windwave dynamics: Marine renewables infrastructure network for emerging energy technologies d2.4. Tech. Rep.; DTU Wind Energy; 2012. Deliverable of the Marinet project.
[23] Hansen, A.M., Laugesen, R.. Experimental study of the dynamic response of the dtu 10mw wind turbine on a tension leg platform. Master's thesis; DTU Wind Energy; 2015.
[24] Yu, W.. Modeling, control design and testing of a scaled floating offshore wind turbine. Master's thesis; University of Stuttgart; 2016.
[25] Lomholt, A.K., Boehm, L.. Implementation of a modelscale floating wind turbine pitch-generator control. Tech. Rep. B-0008; DTU Wind Energy; 2016. BSc Thesis.
[26] Larsen, T.J., Hanson, T.D.. A method to avoid negative damped low frequency tower vibrations for a floating pitch regulated wind turbine. Journal of Physics: Conference Series 2007;75(012073). The Science of Making Torque from Wind.
[27] Hansen, M.H., Hansen, A., Larsen, T.J., Øye, S., Sørensen, P., Fuglsang, P.. Control design for a pitch-regulated, variable-speed wind turine. Tech. Rep. Risø-R-1500(EN); RisøNational Laboratory, Roskilde, Denmark; 2005.
[28] Jonkman, J.M.. Dynamic modeling and loads analysis of an offshore floating wind turbine. Ph.D. thesis; National Renewable Energy Laboratory; Golden, Colorado, US; 2007.
[29] Jonkman, J.M., Musial, S.B.W., Scott, G.. Definition of a 5-MW reference wind turbine for offshore system development. Tech. Rep. NREL-TP500-38060; National Renewable Energy Laboratory; 2009.
[30] Tromans, P.S., Anaturk, A., Hagemeijer, P.. A new model for the kinematics of large ocean waves — application as a design wave. In: Proc. 1st Int. Conf. Offsh. Mech. and Polar Engng. (ISOPE); vol. 3. 1991, p. 64–71.
[31] Lindgren, G.. Some properties of a normal process near a local maximum. Ann Math Stat 1970;41:1870.
[32] Boccotti, P.. Some new results on statistical properties of wind waves. Appl Ocean Res 1983;5:134.
[33] Jonkman, B., Jonkman, J.. Guide to changes in fast v8: v8.12.00a-bjj. Tech. Rep.; National Renewable Energy Laboratory, Golden, Colorado; 2015.